Sirte University Scientific Journal (Applied Sciences) *Vol. 6 (1), 77–88, June 2016*

Features Retard Crack Propagation in Stainless Steels

Farej A. Emhmmed

Faculty of Engineering, University of Ben Walid, Libya
E-mail: Libyatat@yahoo.co.uk

Abstract

The role of some microstructural features in blocking the fracture path was investigated for duplex stainless steels (DSS). Sets of fatigued specimens , Wedge Open Load WOL , were heat treated at 475ºC for different times and pulled to failure either in air , CT specimens , or after kept in 3.5% NaCl with polarization of -900 mV/ SCE i.e. WOL specimens . Fracture took place in general by ferrite cleavage and austenite ductile fracture in transgranular mode. Specimens measured stiffness (Ms) was affected by the aging time, with higher values measured for specimens aged for longer times. The ratio of the measured stiffness to the predicted stiffness was observed to increase with the crack length. Microstructural features played a role in " blocking" the crack propagation process leading to increase the resistance of the material to fracture, R-curve vs. crack length , specially for specimens aged for short times. Unbroken ligaments/ austenite were observed at the crack wake. These features may exerted a shielding stress , blocking effect , at the crack tip giving resistance to the crack propagation process i.e. the crack mouth opening was reduced. Higher stress intensity factor KIC values were observed with increased amounts of crack growth suggesting longer zone of unbroken ligaments in the crack wake. The shielding zone was typically several mm in length.. Attempt to model the bridge stress was suggested to understand the role of ligaments / unbroken austenite in increasing the fracture toughness factor.

Keywords: Fracture toughness, Ligaments , Shielding effect, Stainless steels.

1. Introduction

The austenitic stainless steels are often highly susceptible to localized corrosion attack such as intergranular corrosion in the sensitized condition, and even more to pitting and stress corrosion cracking in the presence of chloride ions [1]. On the other hand, ferritic stainless steels are more sensitive to corrosion than austenitic stainless steels except for stress corrosion cracking in chloride environments and generally have lower weldability [2]. Duplex stainless steels may be defined as a family of steels having a two phase, ferritic-austenitic or austenitic-ferritic, microstructure, the components of which are both stainless

[3]. Duplex stainless steels combine good properties of ferritic steels provides them with excellent resistance to pitting and stress corrosion, high degree of flexibility, resistance to fracture, good tensile strength and in some microstructures superplastic behavior at temperatures of 1100–1300°C . That is why DSS are required in the offshore oil and gas industry. This draws the demand to understand those parameters may control the crack propagation process such as features block / retard the crack tip movements. Pezzotti and Sbaizero [4] studied the shielding stress fields in Al_2O_3/Al composite using a spectroscopic technique based on microprobe measurements of the Cr^{3+} optical fluorescence in the Al_2O_3-matrix phase. Specimens for fracture mechanics tests were parallel pipes 3×4×20mm (B×W×L) in dimension with a straight notch $a_0/W \approx 0.5$ at their Centre. The crack resistance, K_R , was calculated from standard fracture mechanics. The crack-tip toughness, K_{I0} , was calculated from the load value at which the load-displacement curve deviates from linearity. Pezzotti and Sbaizero [4] observed an increase in fracture resistance, K_R with increasing crack length Δa. Scanning electron microscopy observation of the fracture surface revealed Aluminum ligaments stretched between the crack faces indicating extensive occurrence of crack-face shielding during fracture. They proposed that the reduction in stress intensification at the crack tip, the toughness increase, can be expressed in terms of shielding stress intensity factor (ΔK_S) as follows;

$$K_{tip} = K_a - \Delta K_s \qquad (1)$$

Where;

K_{tip} is the stress intensity factor at the crack tip.

K_a is the applied stress intensity factor.

At the critical condition for crack propagation (i.e. for $K_{tip} = K_{I0}$ and $K_a = K_R$) a rising R-curve can be expressed by;

$$K_R = K_{I0} + \Delta K_s \qquad (2)$$

Where ;

K_{I0} is the crack tip toughness. ΔK_S and K_R are functions of the propagation crack length.

The R-curve contribution arising from the shielding stress, σ_{br}, can be calculated from the knowledge of the shielding stress distribution as;

$$K_R = K_{I0} + \sqrt{\frac{2}{\pi}} \int_0^{\Delta a} \frac{\sigma_{br}(x)dx}{\sqrt{x}} \qquad (3)$$

Where

σ_{br} (x) is the shielding stress distribution over the crack extension Δa and the variable x, with origin at the crack tip.

Barinov [5] proposed that since the K_{I0} value does not depend on the crack increment, the mean crack-tip shielding stress, $\Delta\sigma_{br}$, can be expressed in terms of crack length (a) and of the crack-shielding zone increment (Δ_{lb}) if the relationship between the shielding stress distribution, (a) and (Δlb) is known. For a single-edge-notched beam (SENB) , Barinov [5] suggested that equation (2) can be rewritten as follows:

$$K_R - K_I = \Delta\sigma Y a^{\frac{1}{2}} \qquad (4)$$

Where

$$\Delta\sigma = 1.5\frac{\Delta PL}{BW^2} \qquad (5)$$

$$Y = \frac{1.99 - \alpha(1-\alpha)(2.15 - 3.93\alpha + 2.7\alpha^2)}{(1+2\alpha)(1-\alpha)^{\frac{2}{3}}} \qquad (6)$$

ΔP is the load increment due to the crack-tip shielding force.

L , B and W the specimen length, thickness and width respectively.

a is the crack length

$\alpha = a/W$.

Barinov [5] suggested that if the shielding stresses are distributed continuously, an increment of the mean applied stress due to the shielding stresses can be written as;

$$\Delta\sigma = \left(\int_0^{lb} f(\sigma, \Delta l_b)(\Delta l_b) \right) \Big/ \left(a_0 + \int_0^{a} da \right) \qquad (7)$$

Where

L_b is the length of the crack-face shielding zone. $f(\sigma,\Delta l_b)$ is ligament's distribution function. a_0 is initial crack depth. RR In the case of ligaments uniformly distributed along the crack length, the function $f(\sigma, \Delta l_b)$ is supposed to be equal to $(n\sigma_f)$= constant. Accordingly, equation (7) will be;

$$\Delta\sigma = \frac{n\sigma_f \Delta l_b}{a_0 + \Delta a} \qquad (8)$$

Where

(n) is a non-dimensional constant, which accounts for a occupation of a unit of the shielding zone surface by shielding ligaments.

2. Material and Experimental Procedure

Duplex stainless steels , Zeron 100, was used in the wrought state to measure the fracture toughness in terms of K_I for testing in air or K_{ISCC} for environmental assisted cracks .The as-received material was in the form of extruded bars. The material chemical composition is shown in Table 1 . The microstructure for the as received material was with 50:50 ratio the ferrite phase and austenite phase. Specimens from the as-received material were cut perpendicular to the bar axis and were machined into Wedge Open Load , WOL, shape. The (WOL) specimen is self-stressed by the use of a bolt and loading tup. A constant crack

opening displacement is maintained throughout the test, hence the load P, decreases as the crack length increases. Specimens were then fatigued , pre-cracked , for a few millimeters to introduce a sharp crack in front of the notch tip. Heat treatment was conducted to introduce brittleness to the ferrite phase, at 475ºC . Heating time was selected for 2h, 5h, 13h, 24h, 49h, 72h, 166h, 100 and 118h . Finally, specimens were allowed to air-cool to room temperature. Compliance, (load vs. displacement), measurement was carried out for the pre-cracked specimens. Based on the compliance measurement, the COD value required to achieve the required load was calculated. The applied load value was then used to calculate the $K_{applied}$ values as follows [6] :

$$K_I = \frac{PC_3}{B\sqrt{a}} \qquad (9)$$

Where

P= Load .

a = Crack length.

W = Specimen width.

B = Specimen thickness

C3= Function of (a/W) which is given by;

$$C_3\left(\frac{a}{W}\right) = [30.96\left(\frac{a}{W}\right) - 195\left(\frac{a}{W}\right)^2 + 730.63\left(\frac{a}{W}\right)^3 - 1186.3\left(\frac{a}{W}\right)^4 + 754.6\left(\frac{a}{W}\right)^5] \qquad (10)$$

Specimen predicted stiffness , P_S to be compared to the measured stiffness M_S later , , was calculated according to the following equation [5]:

$$V = \frac{PCV}{EB} \qquad (11)$$

Where ;

$$C_V = e^{[1.67247 + 7.70302(\frac{a}{W}) - 6.65972(\frac{a}{W})^2 + 5.95445(\frac{a}{W})^4]} \quad (12)$$

V is the crack open displacement i.e. COD applied / arrest

P laod.

A is the fatigue crack length.

Specimens then were loaded individually to the a chosen $K_{applied}$, by bolt loading as a feature of WOL specimens , and immersed into the test environment which was 3.5wt% NaCl at room temperature. Potentials of –900mV/SCE was used in this investigation. After 14 days specimens were taken out of the test environment and cleaned. The crack opening displacement (COD) was recorded for each specimen before unloading , i.e. COD arrest. The load necessary to achieve the value of COD_{arrest} , was recorded by reloading the specimen to its COD_{arrest} value using the Instron tensile machine which displays the load during loading. The compliance, P vs. COD, was recorded during loading / unloading each specimen for M_S measurements. Finally specimens were unloaded and broken open .

3. Results and Discussion

Fracture surface investigation revealed that cracking took place in most of the specimens transgranular by cleavage of the ferrite matrix and ductile tearing of the austenite. Austenite cracking due to environment attack was observed very rarely . This suggests that austenite mechanically retard cracking by blocking the crack path. Crack blocking by the austenite phase was not observed to change the cracking path from transgranular to intergranular. For (WOL) specimen, under constant displacement, the plastic strain rate during the propagation process will be reduced ER with crack growth.

This is supported by the observation of crack bridging by unbroken ligaments and austenite. It suggests that during stable crack growth a condition of stress equilibrium exists

at the crack tip due to the shielding effect exerted by unbroken austenite at the crack tip. The bridging effect exerted by the unbroken austenite on the crack tip is different from that by ligaments in that it occurs over a fine scale and is likely to vary less between individual test specimens. It may be considered as a microstructure parameter. It is necessary for the austenite to fail for the crack to propagate. As shown in Fig.(1.3), ferrite cracked even without austenite failure suggesting that some of the austenite grains may have fractured when the specimen was broken open. During crack propagation, austenite bridging grains were developed but are broken under high strains caused by crack opening displacement As the amount of crack growth increased, the applied load decreased i.e. load-crack growth relationship for (WOL) specimen. Accordingly, the crack opening displacement and thus the local strains in the austenite decreased to a value which is not enough for the failure of newly formed ligaments/ unbroken austenite i.e. crack shielding effect was produced. Specimens tested at low $K_{applied}$, deliberately, showed no indications of fracture . By definition , K_{arrest} is the value of stress intensity factor under which there is no crack propagation takes place. . However, specimens Ms was significantly higher than the Ps as shown in Fig.(1). The ratio of measured / predicted stiffness (Ms/Ps) was found to increase with the amount of crack growth . Disagreement between the measured and predicted was estimated using the following formula:

$$\text{Disagreement\%} = \frac{M_S - P_S}{P_S} \times 100 \qquad (13)$$

The stiffness disagreement was found to increase with the amount of crack growth as shown in Fig. (2) . This increase became more scattered with increasing crack length. The increase in Ms observed after crack growth is probably due to shielding effect exerted by unbroken ligaments on the crack tip.

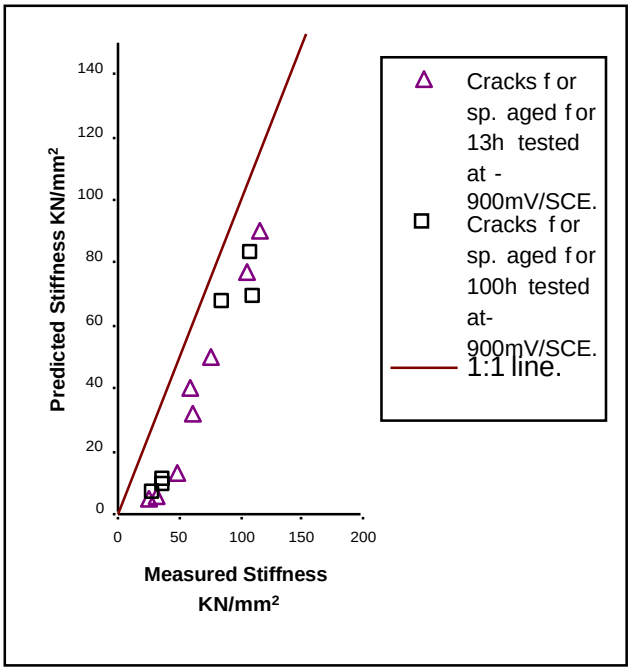

Figure 1. The measured stiffness vs. predicted stiffness for valid SCC cracks

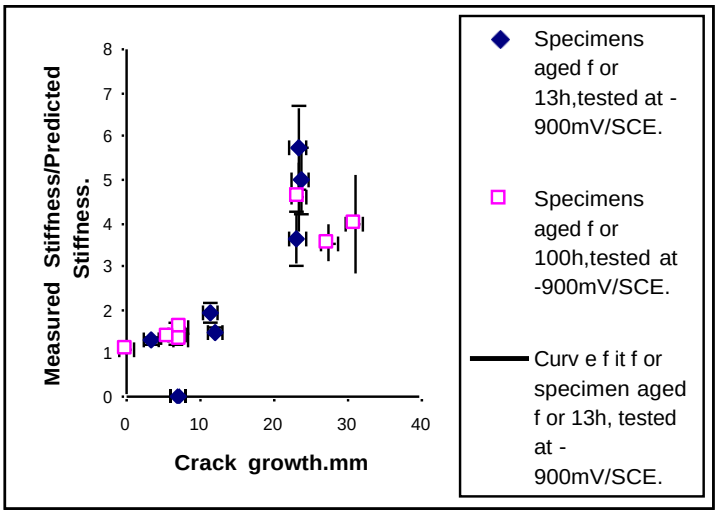

Figure 2. The measured stiffness/ predicted stiffness ratio vs. crack growth

Uncracked austenite/ligaments at the fracture surface exerted bridging effect in crack closure during crack propagation. This will cause the crack mouth not to be open as much as expected and in turn mouth not to be open as much as expected and in turn increases the specimen stiffness . In simple terms, the strain in the bridging austenite grains increases with distance from the crack tip. Therefore as the crack grows, the bridges furthest from the crack tip will fail. Factors that decreased the measured specimen compliance increased the specimen stiffness error.

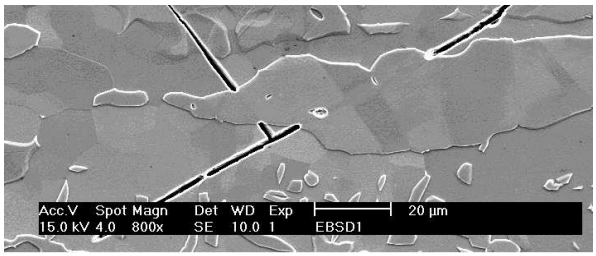

Figure 3. Austenite a crack arrestor observed after SCC for specimen aged at 475ºC for 100h.

Figure 4. SCC crack forking observed for observed Karrest .

The significant change in compliance implied a significant degree of crack shielding, sufficient to cause crack tip shielding. Crack shielding would occur if the applied load was carried partly by the shielding ligaments and not fully transmitted to the crack tip. A simple model for crack tip shielding due to crack shielding may be constructed which assumes that the critical stress intensity factor for crack propagation is the intrinsic threshold stress

intensity factor for the non-bridged crack (K_0) plus the shielding contribution due to an average stress (σ_{sh}) acting over the distance of crack extension (∂a). The increase in crack propagation resistance predicted by this shielding model is consistent with a shielding stress, σ_{sh}, of the order of 300–600 MPa, and an intrinsic K_0 of 40 MPa $m^{1/2}$ (Fig.4). These values represent a shielding stress which is a significant fraction of the tensile yield strength (900 MPa) of the material, and the observed lower bound of the threshold stress intensity for environment- assisted cracking . Equation (15) was used for constructing a raising-R curve for the tested material. As shown in Fig.(5), the K_1 value observed for specimens increased with the amount of crack growth.

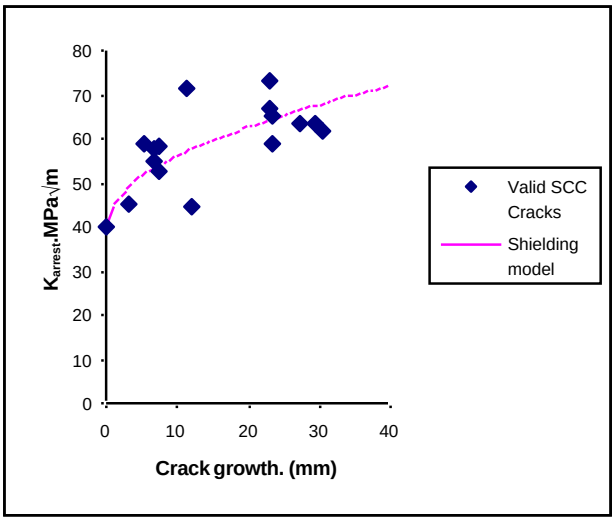

Figure 5. specimen aged at 475ºC for 100h to prediction by shielding model.

The shielding stress , σ_{br} , was assumed to be a constant value along the crack length. Consequently, equation (3) can by written as;

$$K_R = K_{I0} + \sqrt{\frac{2}{\pi}}\,\sigma_{br} \int_0^{\Delta a} \frac{dx}{\sqrt{x}} \qquad (14)$$

$$K_R = K_{I0} + \sqrt{\frac{2}{\pi}}\frac{\sigma_{br}}{2}[\sqrt{\Delta a}] \quad (15)$$

From the general trend of the observed data, the K_{I0} value corresponds to $\Delta a=0$ which was estimated to be 40MPa$\sqrt{m}$. The obtained K_{arrest} R-curve was in good agreement with the model when constant shielding stress equal to 400MPa was used. This value of shielding stress is reasonable since it is in agreement with austenite tensile strength and the 50% area fracture of the austenite in the shielding zone. The lower K_{arrest} /K_{1SCC} value probably is the most important since it represents the intrinsic value. The second term in equation (15) represents crack wake shielding exerted on the tip of a propagating crack. The model is able to predict the K_{arrest} value observed in the present work.

Table 1. The Chemical Composition Of The As-Received Material

Element	Wt %
C	0.02
Si	0.22
Mn	0.58
P	0.021
S	0.001
Cr	25.12
Mo	3.55
Ni	6.90
W	0.54
Cu	0.59
Fe	Bal.

4. Conclusion

- Fracture in duplex stainless steels occurs by ferrite cleavage and austenite ductile tearing.

- The cracking path is transgranular throughout the ferrite phase. - Austenite acts as a crack arrestor and no austenite dissolution was observed.

- Ageing at 475ºC decreases the fracture toughness .
- The threshold intensity factor (K1) increases with amount of crack growth. This is mainly due to shielding effect increases with the crack extension.

- The lowest K1SCC value i.e. 40MPa√m, which assumed to correspond to a material intrinsic resistance to stress corrosion cracking.

A bridging model has been proposed for the shielding effect on stress corrosion cracking mechanism due to ligaments development in the crack wake

5. References

[1] J.E.Truman and K. R.Pirt " Properties Of A Dulpex (Austenitic – Ferritic) Stainless Steel And Effect Of Thermal History *", Duplex stainless steels `83, Conference proceeding . ed. Lula, R.A., ASM* , 1983,PP 113 – 142.

[2] G. Herbsleb and P. Schwaab, " Precipitation of Intermetallic Compounds, Nitrides and Carbides in AF 22 Duplex Stainless Steel and Their Influence on Corrosion Behavior In Acids". *Duplex stainless steels `83 , Conference proceeding ,ed. Lula, R.A., ASM* ,1983, PP15-40.

[3] M.Murata,Y. Mukai and J.Wang, " Susceptibility of Hydrogen Induced Stress Corrosion Cracking of Duplex Stainless Steel and its Welded Jionts in Acids Environment", *Proceedings of EVALMAT 89,© ISIJ*,PP 287-294.

[4] G.Pezzotti and O.Sbaizero , "Residual And Bridging Microstress Fields In AL2O3/Al Interpenetrating Network Composite Evaluated By Fluorescence Spectroscopy" , *Materials Science and Engineering A, Vol.303, 2001,* PP 267-272.

[5] S.M.Barinov , "On Crack-Face Bridging In A Particulate Ceramic-Metal Composite*", J.Mat.Sci.let.,Vol.16, 1997*, PP1827-1829.

[6] BS 7448, Fracture Mechanics Toughness Tests . Part 1 . "Method For Determination Of KIC, Critical CTOD and Critical J Values Of Metallic Materials", *Annual Book Of BSI Standard,* 1991.